Cell, Vol. 115, 139–150, October 17, 2003, Copyright ©2003 by Cell Press

# Nitric Oxide Regulates Exocytosis by S-Nitrosylation of N-ethylmaleimide-Sensitive Factor

**Kenji Matsushita,[1] Craig N. Morrell,[2,3] Beatrice Cambien,[7] Shui-Xiang Yang,[1] Munekazu Yamakuchi,[1] Clare Bao,[1] Makoto R. Hara,[4] Richard A. Quick,[1] Wangsen Cao,[1] Brian O'Rourke,[1] John M. Lowenstein,[6] Jonathan Pevsner,[4,5] Denisa D. Wagner,[7] and Charles J. Lowenstein[1,2,*]**

[1]Department of Medicine
[2]Department of Pathology
[3]Department of Comparative Medicine
[4]Department of Neuroscience and
[5]The Kennedy Krieger Institute
The Johns Hopkins University School of Medicine
Baltimore, Maryland 21205
[6]Department of Biochemistry
Brandeis University
Waltham, Massachusetts 02454
[7]The Center for Blood Research and
Department of Pathology
Harvard Medical School
Boston, Massachusetts 02115

## Summary

**Nitric oxide (NO) inhibits vascular inflammation, but the molecular basis for its anti-inflammatory properties is unknown. We show that NO inhibits exocytosis of Weibel-Palade bodies, endothelial granules that mediate vascular inflammation and thrombosis, by regulating the activity of N-ethylmaleimide-sensitive factor (NSF). NO inhibits NSF disassembly of soluble NSF attachment protein receptor (SNARE) complexes by nitrosylating critical cysteine residues of NSF. NO may regulate exocytosis in a variety of physiological processes, including vascular inflammation, neurotransmission, thrombosis, and cytotoxic T lymphocyte cell killing.**

## Introduction

Nitric oxide (NO) is a messenger molecule produced by the NO synthase (NOS) isoforms neuronal NOS (nNOS, or NOS1), inducible NOS (iNOS, or NOS2), and endothelial NOS (eNOS, or NOS3) (Nathan and Xie, 1994; Stamler et al., 1992). All three NOS isoforms can be found in the vasculature—NOS1 in nerve fibers in the adventitia, NOS2 in vascular smooth muscle cells and in infiltrating macrophages during vascular inflammation, and NOS3 in endothelial cells—and NO has a variety of effects upon vascular cells (Christopherson and Bredt, 1997; Michel and Feron, 1997; Papapetropoulos et al., 1999; Radomski and Moncada, 1993). NO relaxes smooth muscle, inhibits smooth muscle cell migration and proliferation, and decreases platelet adherence and aggregation. NO also inhibits vascular inflammation: atherosclerosis is increased in mice deficient in NOS2 or NOS3, transplant vasculopathy is exacerbated in mice lacking NOS2, and the response to vascular injury is accelerated in NOS3 null mice (Kuhlencordt et al., 2001a, 2001b; Rudic et al., 1998). However, the molecular basis for the anti-inflammatory properties of NO is not completely understood.

NO may regulate vascular inflammation in part by inhibiting exocytosis of Weibel-Palade bodies (Qian et al., 2001). Weibel-Palade bodies are granules rapidly released from endothelial cells that mediate vascular thrombosis and inflammation (Wagner, 1993). Discovered by Weibel and Palade in 1964, Weibel-Palade bodies are cigar-shaped organelles that contain von Willebrand factor (vWF), P-selectin, tissue plasminogen activator, and CD63 (Bonfanti et al., 1989; Huber et al., 2002; McEver et al., 1989; Vischer and Wagner, 1993; Wagner et al., 1982; Weibel and Palade, 1964). Exocytosis of Weibel-Palade bodies leads to the release of vWF, which promotes platelet adhesion and aggregation (Ruggeri, 1997). Weibel-Palade body exocytosis also leads to the translocation of the transmembrane protein P-selectin to the endothelial cell plasma membrane, where it regulates leukocyte rolling and extravasation (Mayadas et al., 1993; McEver et al., 1989). Secretagogues such as thrombin, histamine, fibrin, complement, leukotrienes, and ATP all trigger Weibel-Palade body exocytosis within minutes. Although the molecular machinery regulating Weibel-Palade body exocytosis is not defined, it is likely that proteins that regulate vesicle trafficking in other cells also regulate Weibel-Palade body exocytosis in endothelial cells.

Vesicle trafficking involves targeting of a vesicle to a specific membrane, priming of the vesicle, and membrane fusion, followed by recycling of trafficking components (Jahn et al., 2003; Jahn and Sudhof, 1999; Mellman and Warren, 2000; Rothman and Wieland, 1996; Springer et al., 1999; Wickner and Haas, 2000). At least four classes of proteins regulate membrane fusion: Rab and Rab effectors, which regulate vesicle tethering to target membranes; soluble NSF receptor (SNARE) proteins, which are localized to vesicle and target membranes and assemble into stable ternary complexes; members of the Sec1/Munc18 protein family; and NSF, along with the family of soluble NSF attachment proteins (SNAP), which plays a critical role in regulating vesicle trafficking by hydrolyzing ATP and disassembling SNARE complexes.

NSF was first identified as a cytosolic protein necessary for in vitro reconstitution of intercisternal Golgi transport, and subsequently was shown to regulate intracellular transport in yeast, nematodes, insects, and mammals (Block et al., 1988; Kaiser and Schekman, 1990; Malhotra et al., 1988; May et al., 2001). NSF forms homohexamers, hydrolyzes ATP, and alters the conformation of the stable SNARE complex (Block et al., 1988; Malhotra et al., 1988). NSF is composed of three domains: an N-terminal domain and two homologous ATP binding domains. The N-terminal domain (residues 1–205) interacts with members of the SNAP family, which in turn interact with SNARE molecules. The D1 domain (resi-

*Correspondence: clowenst@jhmi.edu

dues 206–488) hydrolyzes ATP and provides the mechanical force to disassemble SNARE complexes. The D2 domain (residues 489–744) mediates NSF hexamerization.

Although NSF regulates vesicle trafficking and exocytosis, the regulation of NSF is not well understood. Sensitivity to NEM suggests that NSF might be regulated by S-nitrosylation, a mechanism by which NO modulates protein functions (Stamler, 1994; Stamler et al., 2001, 1992). We hypothesized that NO regulates exocytosis by nitrosylating NSF. We show that NO inhibits Weibel-Palade body exocytosis from endothelial cells, in part by inhibiting NSF disassembly activity.

## Results

### Exogenous and Endogenous NO Inhibits Weibel-Palade Body Exocytosis

To explore the effect of NO upon granule exocytosis, we studied thrombin-induced exocytosis of Weibel-Palade bodies from human aortic endothelial cells (HAEC), which release von Willebrand's Factor (vWF). We pretreated HAEC with 10 mM NO donor 2-(N,N-diethylamino)-diazenolate-2-oxide (DEA-NONOate) or with DEA as a control, stimulated the cells with thrombin 1 U/ml for 1 hr, and then measured the amount of vWF released into the media. Thrombin induces a rapid release of vWF from HAEC (Figure 1A). However, exogenous NO blocks the effects of thrombin (Figure 1A). Endogenous NO produced from endothelial cells also inhibits vWF release, since 1 mM L-nitroarginine-methyl-ester (L-NAME) inhibition of NOS for 16 hr increases the amount of vWF released after thrombin stimulation (Figure 1A). NO inhibition of vWF release is dose dependent. We pretreated HAEC with increasing amounts of various NO donors, including a rapidly releasing NO donor DEA-NONOate for 10 min, a slowly releasing NO donor DETA-NONOate for 16 hr, or a nitrosothiol S-nitroso-penicillamine (SNAP) for 6 hr; or we treated cells with NEM for 1 hr. Pretreatment with any one of these reagents inhibits thrombin induced vWF release (Figure 1B).

We then explored the role of endogenous NO in the regulation of Weibel-Palade body exocytosis. We pretreated HAEC with L-NAME for 16 hr in order to inhibit endogenous NOS and then stimulated the cells with 1 U/ml thrombin for 1 hr and measured vWF release. L-NAME increases thrombin-stimulated vWF release in a dose-dependent manner (Figure 1C). (The iNOS inhibitor 1400W had no effect [data not shown]). We next pretreated HAEC with vascular endothelial growth factor (VEGF) in order to activate endogenous NOS3. Cells were incubated with 50 ng/ml VEGF or control for 2 hr, and then stimulated with thrombin. VEGF treatment decreases thrombin stimulated vWF release (Figure 1D). L-NAME 1 mM blocks the effects of VEGF treatment, implying that NO mediates VEGF inhibition of exocytosis (Figure 1D). Since L-NAME inhibition of NOS increases exocytosis and since VEGF activation of NOS decreases exocytosis, taken together, these data suggest that endogenous NO regulates endothelial cell exocytosis.

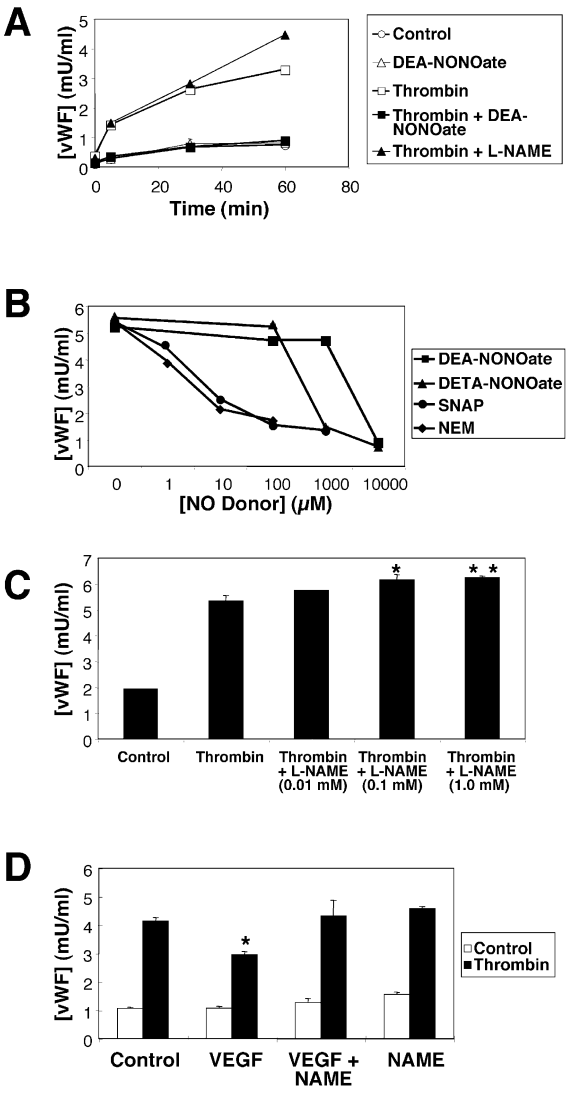


Figure 1. NO Inhibits vWF Release from Human Aortic Endothelial Cells

(A) Time course. HAEC were pretreated with DEA as a control or the NO donor DEA-NONOate or the NOS inhibitor L-NAME, and then incubated with thrombin for 1 hr. The amount of vWF released from cells into the media was measured by an ELISA ($n = 3–5 \pm SD$). Exogenous NO inhibits exocytosis, and L-NAME inhibition of endogenous NOS increases exocytosis.

(B) Dose response. HAEC were pretreated with DEA-NONOate for 10 min, DETA-NONOate for 16 hr, SNAP for 6 hr, or NEM for 1 hr and then incubated with thrombin for 1 hr. The amount of vWF released from cells was measured by an ELISA ($n = 3–5 \pm SD$).

(C) Inhibition of endogenous NOS increases vWF release. HAEC were pretreated with L-NAME for 16 hr, incubated with thrombin for 1 hr, and vWF released from cells was measured as above ($n = 2 \pm SD$, $^*p < 0.06$ versus thrombin; $^{**}p = 0.03$ versus thrombin).

(D) Activation of endogenous NOS decreases vWF release. HAEC were pretreated with media or 1 mM L-NAME for 16 hr, stimulated with 50 ng/ml VEGF for 2 hr, and then incubated with thrombin. The amount of released vWF was measured as above ($n = 3 \pm SD$, $^*p < 0.01$ versus control).

### SNARE Molecules Regulate Weibel-Palade Body Exocytosis

The molecular machinery that regulates Weibel-Palade body exocytosis is unknown. However, since SNARE molecules regulate exocytosis of vesicles and granules from other cells, we reasoned that they might also regulate endothelial cell exocytosis of Weibel-Palade bodies

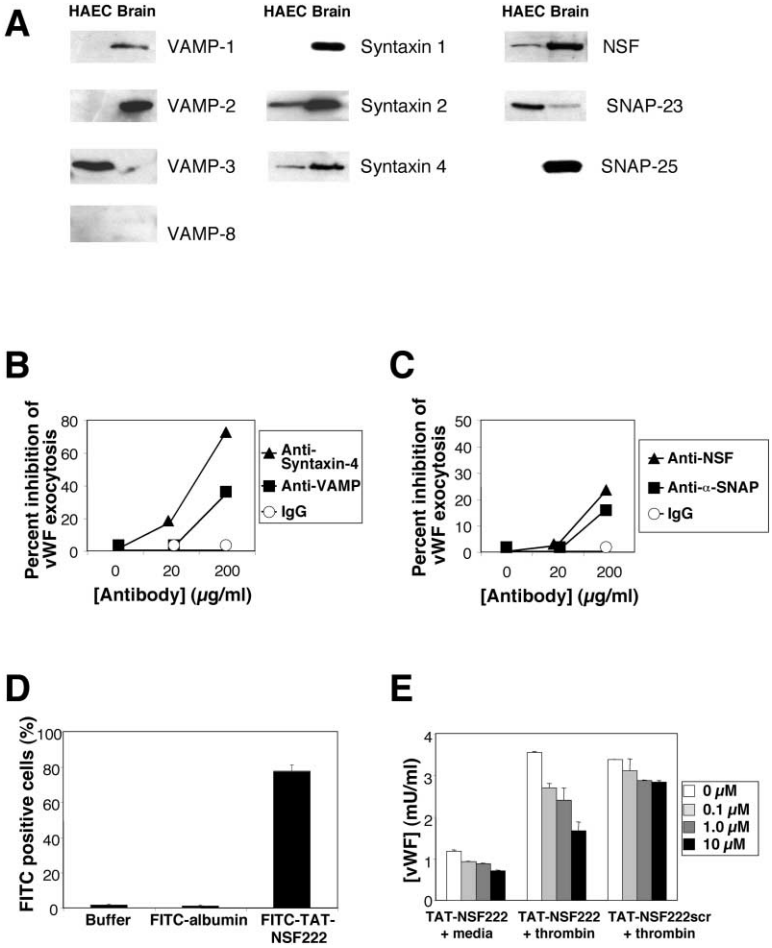


Figure 2. NSF and SNARE Molecules Regulate Weibel-Palade Body Secretion

(A) NSF and SNARE molecules are expressed in endothelial cells. Immunoblotting of 200 μg extracts of endothelial cells or human brain with antibodies to NSF and SNARE molecules.

(B) Antibodies to SNARE molecules inhibit Weibel-Palade body exocytosis. HAEC were permeabilized and incubated with antibodies to SNARE molecules. Cells were then resealed, treated with thrombin, and the amount of vWF released into the media was measured by ELISA (n = 2).

(C) Antibody to NSF inhibits Weibel-Palade body exocytosis. HAEC were permeabilized and incubated with antibody to NSF or α-SNAP. Cells were then resealed, treated with thrombin, and the amount of vWF released was measured as above (n = 2).

(D) NSF peptides enter HAEC. Cells were incubated with FITC-labeled TAT-NSF peptide for 20 min, treated with ethidium bromide to quench extracellular FITC, and imaged by FACS (n = 3 ± SD).

(E) NSF peptides inhibit vWF release. Cells were incubated with TAT-NSF peptides for 20 min, treated with media (left) or thrombin (middle and right), and the amount of released vWF was measured (n = 3 ± SD).

as well. We first determined the expression of SNARE molecules in endothelial cells, using brain extracts as a control. HAEC and human brain extracts were immunoblotted with antibodies to SNARE molecules. HAEC express VAMP-3, syntaxin-2 and syntaxin-4, and SNAP-23 (Figure 2A). To explore the role of syntaxin-4 and VAMP-3 in the regulation of vWF release, we permeabilized HAEC and then incubated them with antibody to syntaxin-4, antibody to VAMP, or IgG as a control. Cells were then resealed, treated with thrombin, and the amount of vWF released into the media was measured. Antibody to syntaxin-4 inhibits vWF release by over 75% (Figure 2B). Antibody that reacts with VAMP isoforms 1, 2, and 3 inhibits vWF release by approximately 25%. These results suggest that SNARE molecules regulate Weibel-Palade body exocytosis.

### NSF Regulates Weibel-Palade Body Exocytosis

We next explored the role of NSF in regulating Weibel-Palade body exocytosis. We first determined that HAEC express NSF (Figure 2A). We then used two approaches to show that NSF regulates Weibel-Palade body exocytosis. Our first approach involved antibody inhibition of exocytosis. We permeabilized HAEC as above, incubated cells with antibody to NSF or antibody to α-SNAP, resealed the cells, and stimulated them with thrombin. Antibody to NSF inhibits vWF release by approximately 25% (Figure 2C). Antibody to α-SNAP also inhibits vWF release.

Our second approach to demonstrating NSF regulation of Weibel-Palade body exocytosis involved peptide inhibition of NSF. We designed a peptide inhibitor of NSF that crosses cell membranes. This peptide, designated TAT-NSF222, consists of the protein transduction domain of HIV TAT (residues 47–57) previously shown to transduce polypeptides into cells (Becker-Hapak et al., 2001) fused to a fragment of NSF (residues 222–243) previously shown to inhibit NSF (Schweizer et al., 1998). To show that this peptide enters HAEC, we incubated HAEC with 10 μM FITC-labeled TAT-NSF or 10 μM FITC-albumin for 20 min, added ethidium bromide to quench extracellular fluorescence, and analyzed fluorescence of the cells by FACS. Over 75% of cells treated with FITC-TAT-NSF222 contained FITC (Figure 2D). We then incubated HAEC for 20 min with TAT-NSF222 or with a control peptide TAT-NSF222scr that consisted of the intact TAT domain followed by the amino acid residues of NSF 222-243 in a scrambled order. HAEC were transduced with TAT-NSF peptides, treated with media or thrombin, and the amount of vWF released into the media was measured by ELISA. TAT-NSF222 inhibits vWF release in a dose-dependent manner (Figure 2E).

Taken together, the antibody and peptide inhibition data suggest that NSF regulates Weibel-Palade body exocytosis.

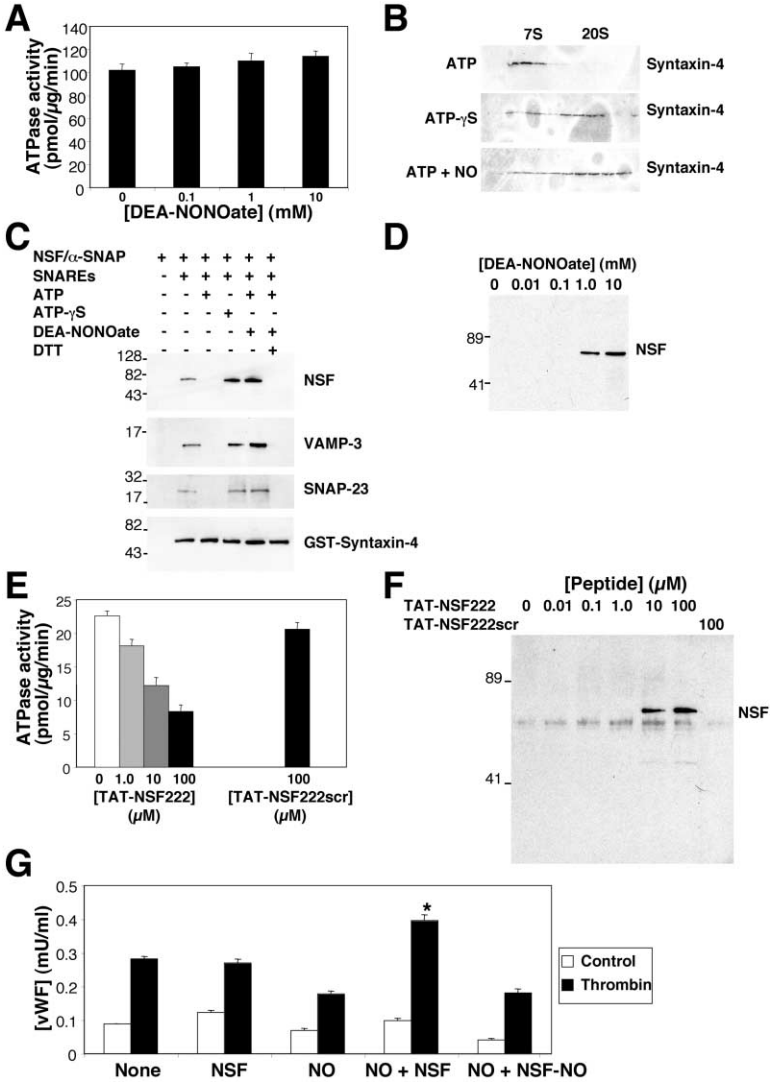


Figure 3. NO Inhibition of NSF

(A) NO does not inhibit NSF ATPase activity. A colorimetric assay was used to measure the ATPase activity of recombinant NSF that had been treated with DEA-NONOate (n = 3 ± SD).

(B) NO inhibits NSF disassembly of 20S complex. Recombinant NSF was pretreated or not with 1 mM DEA-NONOate for 10 min, mixed with α-SNAP, and added to detergent extracts of HAEC membranes. ATP or ATP-γS 0.5 mM was added, and the mixture was fractionated by ultracentrifugation. Fractions were collected from the bottom of the tubes and immunoblotted with antibody to syntaxin-4.

(C) NO inhibits NSF disassembly activity. Recombinant $(His)_6$-NSF was pretreated or not with 1 mM DEA-NONOate and then incubated with α-SNAP, VAMP-3, SNAP-23, and GST-syntaxin-4. ATP or ATP-γS 5 mM was added, the mixture was precipitated with glutathione-sepharose, and precipitated proteins were immunoblotted with antibodies as indicated.

(D) NO inhibits NSF disassembly activity: dose response. Recombinant NSF was pretreated with DEA-NONOate for 10 min, mixed with α-SNAP, and added to endothelial cell GST-SNARE fusion polypeptides as above. ATP 5 mM was added, GST-SNAREs were precipitated with glutathione-sepharose, and the precipitant was analyzed for the coprecipitation of NSF.

(E) TAT-NSF peptides inhibit NSF ATPase activity. A colorimetric assay was used to measure the ATPase activity of recombinant NSF that had been treated with TAT-NSF peptides.

(F) TAT-NSF peptides inhibit NSF disassembly activity. Recombinant NSF was pretreated with TAT-NSF peptides for 20 min and mixed with α-SNAP and endothelial cell GST-SNARE fusion polypeptides as above. ATP was added, GST-SNAREs were precipitated with glutathione-sepharose, and the precipitant was analyzed for the coprecipitation of NSF.

(G) Exogenous NSF restores vWF exocytosis in endothelial cells treated with NO. HAEC were pretreated with 1 mM DEA-NONOate as above, permeabilized with SLO, incubated with recombinant NSF or nitrosylated recombinant NSF, stimulated with thrombin, and the amount of vWF in the media was measured (n = 3 ± SD, *p < 0.01 for NO versus NO + NSF).

### NO Does Not Inhibit NSF ATPase Activity

We next explored the effect of NO upon NSF activity since NO inhibits Weibel-Palade body exocytosis and since NSF regulates Weibel-Palade body exocytosis. We first examined the effect of NO upon the ATPase activity of NSF. DEA-NONOate was added to recombinant NSF, and the ATPase activity of NSF was measured. NO does not significantly inhibit NSF hydrolysis of ATP (Figure 3A).

### NO Inhibits NSF Disassembly Activity

We next explored the effect of NO upon NSF disassembly activity. ATP is required for NSF to disassemble the SNARE complex; ATP-γS can lock NSF onto the SNARE complex. The SNARE complex alone sediments at 7S, and the NSF-α-SNAP-SNARE complex sediments at approximately 20S. Accordingly, we pretreated recombinant NSF with the NO donor DEA-NONOate 1 mM for 10 min. We then mixed pretreated NSF, α-SNAP, and detergent extracts of HAEC membranes in the presence of 0.5 mM ATP or ATP-γS. These reactions were then fractionated by sucrose density gradient ultracentrifugation and fractions were collected from the bottom of the tube and immunoblotted with antibody to syntaxin-4. The SNARE complex sediments at 7S, as expected in the presence of NSF and ATP (Figure 3B, top). The SNARE complex sediments at 20S, as expected in the presence of NSF and ATP-γS (Figure 3B, middle). However, the SNARE complex also sediments at 20S in the presence of ATP and NSF pretreated with DEA-NONOate (Figure 3B, bottom). These results suggest that NO inhibits the ability of NSF to disassemble a 20S SNARE complex derived from endothelial cell extracts.

We next examined the effect of NO upon NSF disassembly of purified, recombinant SNARE molecules. Recombinant $(His)_6$-NSF was pretreated or not with 1 mM DEA-NONOate for 10 min and then mixed with $(His)_6$-α-SNAP and recombinant SNARE fusion polypeptides

identified in endothelial cells: GST-syntaxin-4, VAMP-3, and SNAP-23. ATP or ATP-γS was added, the mixture was precipitated with glutathione-sepharose beads, and precipitated proteins were fractionated by SDS-PAGE and immunoblotted with antibody to the NSF tag.

NSF with α-SNAP interacts with GST-syntaxin-4 (Figure 3C). ATP decreases the interaction of NSF with GST-syntaxin-4; ATP also decreases the coprecipitation of VAMP-3 and SNAP-23 along with GST-syntaxin-4, presumably by NSF disassembly of the SNARE complex. As expected, ATP-γS blocks NSF disassembly activity. However, NO blocks NSF disassembly of the SNARE complex, even in the presence of ATP (Figure 3C). Furthermore, DTT restores the disassembly activity of NSF pretreated with NO, suggesting that NO inhibition of NSF disassembly is reversible. Finally, NO inhibits NSF disassociation from GST-syntaxin-4 in a dose-dependent manner (Figure 3D).

(The low level of interaction between NSF and SNAREs in the absence of adding additional ATP to the reaction mixture may be due to residual ATP in the storage buffer used to prepare recombinant NSF. Small amounts of ATP present in the reaction buffer may permit an interaction between NSF and SNAREs, while larger amounts enable NSF to disassemble the SNARE/α-SNAP/NSF complex.)

### TAT-NSF Peptides Inhibit NSF ATPase Activity and NSF Disassociation from SNAREs

NO and TAT-NSF peptides inhibit NSF by different mechanisms. NO inhibits NSF disassembly activity but does not affect NSF ATPase activity, as shown above. In contrast, the TAT-NSF222 peptide inhibits both NSF ATPase activity (Figure 3E) and also NSF disassembly activity (Figure 3F). Thus, the mechanisms by which NO and TAT-NSF peptides inhibit NSF are different: both inhibit NSF disassembly activity, but only TAT-NSF peptides inhibit NSF ATPase activity as well. Since NO reversibly inhibits NSF disassembly activity without affecting its ATPase activity, we reasoned that NO targets NSF cysteine residues in regions of NSF that couple the energy of ATP hydrolysis to the mechanical energy of disassembling the SNARE complex.

### NO Inhibits Exocytosis by Inhibiting NSF

To confirm that NSF is a primary physiological target of NO, we pretreated HAEC with 1 mM DEA-NONOate for 10 min to inhibit exocytosis, permeabilized the endothelial cells as above, and then added recombinant NSF 100 μg/ml. HAEC were then resealed, stimulated with thrombin, and the amount of vWF released into the media was measured. As before, NO inhibits exocytosis (Figure 3G). However, exogenous recombinant NSF restores the ability of NO treated HAEC to undergo exocytosis (Figure 3G). In contrast, recombinant NSF pretreated with NO cannot restore the ability of NO treated HAEC to undergo exocytosis (Figure 3G). These data suggest that NSF is indeed a primary target of NO in cells.

### Cysteine Residues Mediate NSF Activity

NSF contains 9 cysteine residues, 3 in the N-terminal domain, 3 in the D1 domain, and 3 in the D2 domain (Figure 4A). To determine the importance of individual cysteine residues in NSF functions, we made nine individual NSF mutants, each lacking one of the nine cysteine residues, and then compared the activity of wild-type NSF to mutant NSF.

We first determined which cysteine residues mediate NSF ATPase activity. We measured the ATPase activity of wild-type NSF and of each NSF mutant. Mutation of cysteine residues 21, 91, 264, and 334 partially decrease NSF ATPase activity (Figure 4B, white bars).

We next determined which cysteine residues mediate NSF interactions with SNARE molecules. We repeated the pull-down assay with wild-type and mutant NSF. NSF and α-SNAP were incubated with GST-SNARE fusion polypeptides in the presence of ATP or ATP-γS, and the mixture was precipitated with glutathione-sepharose beads, and finally, immunoblotted with antibody to the NSF tag. Wild-type NSF interacts with GST-SNAREs in the presence of ATP-γS and disassembles GST-SNAREs in the presence of ATP (Figure 4C). Mutation of cysteine residues 250 and 599 have no effect on NSF interaction and disassembly activity. Mutation of cysteine residues 11, 21, 334, 568, and 582 block the ability of NSF to interact with GST-SNARE molecules. Mutation of cysteine residues 91 and 264 permit NSF to interact with the SNARE complex, but inhibit the ability of NSF to disassemble the GST-SNARE complex. These data suggest that one set of NSF cysteine residues regulate NSF interactions with SNARE complexes and another set of NSF cysteine residues regulate NSF disassembly of SNARE complexes. In particular, cysteine residues 91 and 264 appear to regulate NSF disassembly activity.

### NSF Cysteine Residue Targets of NO

We next used these NSF cysteine mutants to explore which cysteine residues of NSF are targets of NO. We added NO to wild-type and mutant NSF and measured the ATPase activity. NO does not affect ATPase activity of wild-type NSF and does not affect ATPase activity of any of the NSF mutants (Figure 4B, black bars).

We then tested the effect of NO upon the disassembly activity of NSF mutants, using the pull-down assay. NO blocks the ability of wild-type NSF to disassemble the SNARE complex in the presence of ATP (Figure 4C). Mutation of cysteine residues 250 and 599 have no effect on the ability of NO to inhibit NSF disassembly activity. The effect of NO upon cysteine residues 11, 21, 334, 568, and 582 cannot be ascertained, since mutation of these residues abrogates NSF interaction with SNARE molecules. Mutation of cysteine residues 91 and 264 blocks the ability of NSF to disassemble the SNARE complex, and NO has no effect upon these mutants.

We next measured the number of cysteine residues that are nitrosylated by exogenous NO. We exposed recombinant NSF to increasing amounts of DEA-NONOate and then used the Saville reaction to measure the number of nitrosocysteine residues per molecule of NSF. NO nitrosylates NSF in a dose-dependent manner (Figure 4D). At 1 mM DEA-NONOate, approximately 3 cysteine residues are modified by NO per each molecule of NSF. (This dose of 1 mM DEA-NONOate also inhibits NSF disassembly activity (Figure 3D).)

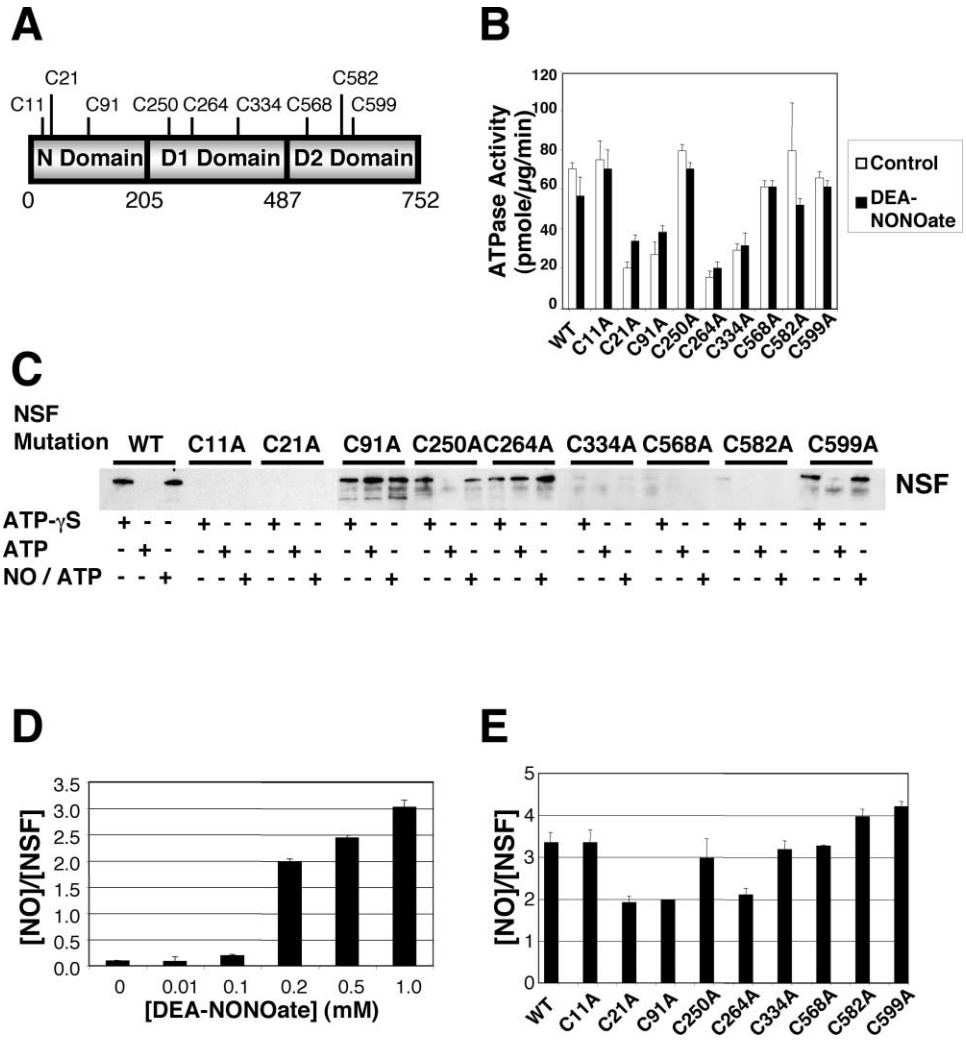


Figure 4. Cysteine Residues Mediating NSF Activity

(A) Schematic of NSF.

(B) Cysteine residues mediating ATPase activity of NSF. Wild-type NSF and mutant NSF were expressed and purified, treated with 1 mM DEA-NONOate or DEA, and the ATPase activity was measured as above. Mutagenesis of Cys at 21, 91, 264, and 334 partially inhibits NSF ATPase activity. NO does not inhibit ATPase activity of wild-type or mutant NSF (n = 3 ± SD).

(C) Cysteine residues mediating disassembly activity of NSF. Wild-type NSF and mutant NSF (with mutated Cys residues) were expressed and purified, and disassembly activity was measured by the pull-down assay as above. Mutagenesis of Cys at 11, 21, 334, 568, and 582 inhibits NSF interaction with SNARE complex. Mutagenesis of Cys at 91 and 264 permits NSF interaction with SNARE complex but blocks NSF disassembly of SNARE complex. Mutagenesis of Cys at 250 and 599 has no effect on NSF interaction or disassembly.

(D) Nitrosylation of NSF in vitro. DEA-NONOate was added to recombinant wild-type NSF, and the molar ratio of nitrosothiols per NSF molecule was measured by the Saville reaction. Each molecule of NSF can contain a maximum of three nitrosothiols (n = 3 ± SD).

(E) Identification of nitrosylated cysteine residues in NSF. DEA-NONOate was added to recombinant NSF mutants, and the molar ratio of nitrosothiols per NSF molecule was measured by the Saville reaction. Mutation of C21 or C91 or C264 decreases the nitrosothiol content of nitrosylated NSF (n = 3–5 ± SD).

We next identified the cysteine residues that are targets of NO by measuring the number of cysteines that are nitrosylated in wild-type and mutant NSF. DEA-NONOate was added to wild-type or mutant NSF that lack specific cysteine residues, and the Saville reaction was used to measure the number of nitrosocysteine residues per molecule of NSF. Mutation of cysteine residues 11, 250, 334, and 568 have no effect upon the nitrosocysteine content (Figure 4E). However, mutation of cysteine residues 21, 91, or 264 decreases the nitrosocysteine content per NSF molecule by one (Figure 4E). These data suggest that NO nitrosylates cysteine residues 21, 91, and 264 of NSF.

### NO Nitrosylation of NSF Is Reversible

Since NSF plays a general role in vesicle trafficking, permanent inactivation of NSF would slow vesicular trafficking in general. However, local production of NO at the plasma membrane and reversible nitrosylation of NSF could provide spatial regulation of NSF. In order to measure how long NO inhibition of exocytosis lasts, we pretreated HAEC with the NO donor SNAP 100 μM for

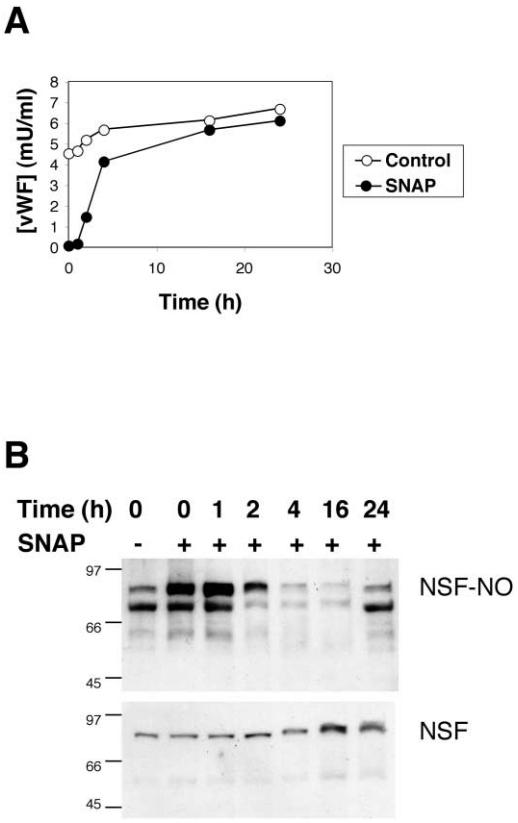


Figure 5. NO Inhibition of Exocytosis and Nitrosylation of NSF Is Reversible

(A) NO inhibition of exocytosis is temporary. HAEC were pretreated with the NO donor SNAP 100 μM for 4 hr, washed to remove the NO donor, and then, at various times after NO treatment, thrombin was added for 1 hr, and the amount of vWF released into the media was measured (n = 3 ± SD).

(B) NO nitrosylation of NSF is reversible. HAEC were pretreated with the NO donor SNAP 100 μM for 4 hr, washed to remove the NO donor, and cells were harvested at various times after treatment. (Top) Cell lysates were immunoprecipitated with antibody to nitrosocysteine and immunoblotted with antibody to NSF. (Bottom) Total cell lysates were immunoblotted with antibody to NSF (this experiment was repeated twice with similar results).

4 hr, washed the cells to remove the NO donor, and then at various times afterwards stimulated the HAEC with thrombin and measured the amount of vWF released into the media. NO inhibits thrombin-induced release of vWF, and a single application of NO continues to inhibit exocytosis 1 hr after treatment (Figure 5A). However, NO inhibition of exocytosis gradually decreases after 1–2 hr; and 2–4 hr after NO treatment about 75% of Weibel-Palade body exocytosis is restored (Figure 5A). Thus, NO inhibition of exocytosis is reversible.

In order to examine directly the reversibility of NSF nitrosylation, we pretreated endothelial cells with an NO donor as above and then harvested cell lysates at various times after NO treatment. Cell lysates were immunoprecipitated with antibody to nitrosocysteine, fractionated by SDS-PAGE, and immunoblotted with antibody to NSF. Treatment with NO increases the level of nitrosylated NSF (Figure 5B, top: − versus + at 0 hr). The level of nitrosylated NSF decreases 2 hr after treatment with NO, and 2–4 hr after treatment the level of nitrosylated NSF is similar to nontreated cells (Figure 5B, top). (In addition to the expected signal for NSF at 82 kDa, another band at approximately 70 kDa is observed.) Treatment with NO donors does not change the total amount of NSF for the first 4 hr, but total amounts of NSF increase 4–16 hr after NO treatment (Figure 5B, bottom).

Taken together, these data show that within 2-4 hr of exposure to NO, nitrosylation of NSF, and inhibition of endothelial cell exocytosis is reversible.

### NSF Is Nitrosylated and Regulates Exocytosis In Vivo

In order to test whether or not NO modifies NSF in vivo, we prepared cell lysates from HAEC treated with media or the NOS inhibitor L-NAME. Polypeptides in this lysate containing nitrosothiols were biotinylated, precipitated with avidin-agarose, and immunoblotted with antibody to NSF (Jaffrey et al., 2001). NSF is nitrosylated in endothelial cells, and treatment of cells with increasing amounts of NOS inhibitor decreases NSF nitrosylation (Figure 6A). We next searched for nitrosylated NSF in mice. Polypeptides were prepared from spleens of wild-type and eNOS null mice as above. NSF is nitrosylated in wild-type mice expressing eNOS (Figure 6B). In contrast, NSF is not nitrosylated in eNOS-deficient mice. These data show that NO nitrosylates NSF in vivo.

To explore the physiological relevance of NSF regulation of Weibel-Palade body exocytosis, we measured the effect of the NSF inhibitory peptide upon the bleeding time in mice. Anesthetized mice were injected intravenously with saline, TAT-NSF222, or the control peptide TAT-NSF222scr; after 45 min, the distal 5 mm of tail was amputated and the bleeding time measured (if the animals bled continuously for 20 min, the experiment was stopped, and the bleeding time was recorded as 20 min). Treatment with saline or the control peptide has no effect upon bleeding time (Figure 6C). In contrast, treatment with TAT-NSF222 dramatically prolongs the bleeding time (Figure 6C). In fact, three of the six mice treated with the TAT-NSF222 peptide had bleeding times in excess of 20 min. (The NSF inhibitory peptides did not enter platelets and did not affect platelet exocytosis [data not shown]. The NSF inhibitory peptides also did not affect vascular contractility of mouse aortas perfused in organ baths [data not shown]). These data show that NSF regulates Weibel-Palade body exocytosis in vivo and suggest that NSF is a novel target for treatment of thrombotic and cardiovascular diseases.

### NO Regulates Exocytosis In Vivo

We explored the physiological relevance of NO regulation of Weibel-Palade body exocytosis in two murine models. We measured the bleeding time in wild-type and eNOS-deficient mice. Lack of eNOS decreases the bleeding time in mice, which would be predicted if a lack of NO decreased NSF inhibition and permitted an increase in exocytosis of vWF (Figure 6D). We also measured serum levels of vWF and soluble P-selectin in wild-type and eNOS-deficient mice. Serum levels of vWF are higher in eNOS-deficient mice compared to wild-type mice (20 ± 25 versus 11 ± 14 mU/ml, although these differences are not significant for n = 6). Serum

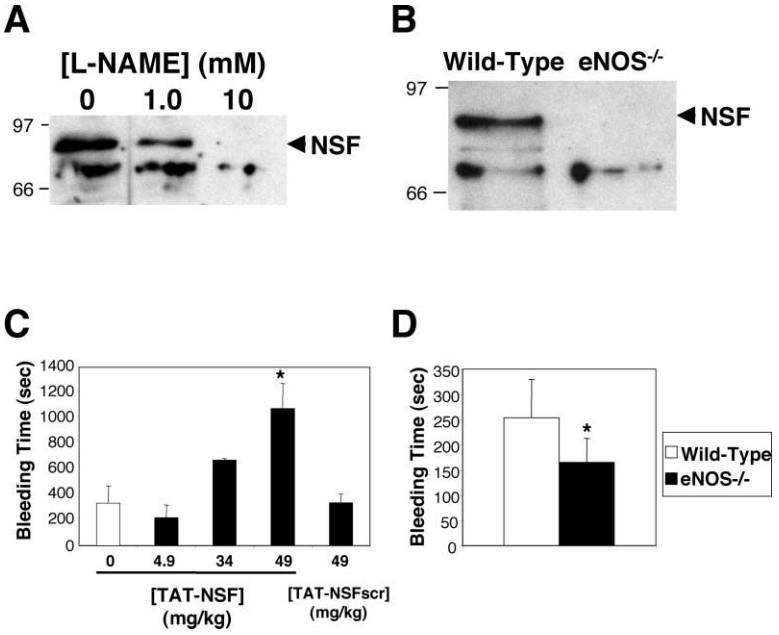


Figure 6. NSF Is Nitrosylated and Inhibits Exocytosis In Vivo

(A) Nitrosylation of NSF in human endothelial cells. HAEC were treated with media alone or the NOS inhibitor L-NAME. Nitrosothiols were biotinylated, precipitated with avidin-agarose, and precipitants were immunoblotted with antibody to NSF. L-NAME inhibits endogenous nitrosylation of NSF in human endothelial cells.

(B) Nitrosylation of NSF in mice. Spleens from wild-type mice and mice lacking eNOS were harvested. Nitrosothiols were biotinylated, precipitated with avidin-agarose, and precipitants were immunoblotted with antibody to NSF. NSF is nitrosylated only in mice expressing eNOS.

(C) Inhibition of NSF in mice prolongs bleeding time. Anesthetized mice were injected with PBS or the TAT-NSF222 peptide that inhibits NSF, and after 45 min, the distal tip of the tail was amputated and the bleeding time was measured. Bleeding that continued longer than 20 min was recorded as 20 min ($n = 3–6 \pm SD$, $^*p < 0.01$ for TAT-NSF versus TAT-NSFscr at 49 mg/kg).

(D) Endogenous NO prolongs bleeding time in mice. The distal tip of the tail was amputated from wild-type and eNOS null mice, and the bleeding time was measured ($n = 7–8 \pm SD$, $^*p = 0.01$ for wild-type versus eNOS null).

levels of soluble P-selectin are also higher in eNOS-deficient mice compared to wild-type mice (81 ± 21 versus 73 ± 14 mU/ml, although these differences are not significant for n = 8). Conclusions from this physiological model of bleeding are limited because NO has effects upon platelets as well as endothelial cells. Despite the limitations of this in vivo model, increased levels of vWF and soluble P-selectin and decreased bleeding times would be expected in eNOS–deficient mice, if NO inhibits exocytosis in vivo.

To further examine the physiological relevance of NO regulation of Weibel-Palade body exocytosis, we measured the effect of endogenous NO upon platelet interactions with endothelial cells in vivo. Platelet rolling, or transient adherence of platelets to the walls of blood vessels, is mediated by vWF released by exocytosis (Andre et al., 2000). We hypothesized that inhibition of endogenous NO synthesis would permit an increase in Weibel-Palade body exocytosis, an increase in released vWF, and an increase in platelet adherence to venule walls. We first showed that exogenous NO can inhibit histamine-induced exocytosis from HAEC (Figure 7A). We next employed intravital microscopy to explore the effects of endogenous NO upon platelet rolling in vivo. Anesthetized mice were pretreated or not with L-NAME and then transfused with calcein-AM labeled platelets. The mesentery was externalized, superfused with histamine, and intravital microscopy was used to record interactions of fluorescently labeled platelets with mesenteric venules. Platelets were classified as adherent if they were transiently captured by the endothelium and then translocated in a stop-and-go fashion for a minimum of 2 s. Histamine rapidly induces platelet adhesion to the venule wall without aggregation, starting within 30 s and peaking 3 min after histamine treatment (Figures 7B and 7C). Inhibition of endogenous NOS with L-NAME increases histamine-induced platelet interactions with the venule wall to a frequency more than double that observed in nontreated mice (Figures 7B and 7C). Furthermore, inhibition of endogenous NOS permits an increase in platelet-venule interactions, which finally peaks at 6 min after histamine treatment, indicating that the vWF release continues twice as long as in the control mice. This increase in transient platelet adherence to the venule would be predicted if less NO synthesis led to increased exocytosis of Weibel-Palade bodies and more release of vWF.

The bleeding time and platelet rolling data taken together suggest that NO regulates hemostatically important granule secretion in vivo.

## Discussion

The major finding of this study is that NO regulates exocytosis by nitrosylating NSF, thereby inhibiting NSF disassembly activity. Inhibition of NOS increases endothelial release of vWF and increases platelet adherence to the stimulated vessel wall. Although NSF was originally purified as a protein necessary for intercisternal Golgi transport that was inhibited by NEM, our data suggests that NEM-Sensitive Factor is actually an NO-Sensitive Factor.

### How Does NO Inhibit NSF?

NO regulates a wide variety of proteins by nitrosylation of critical cysteine residues (Stamler, 1994; Stamler et al., 2001, 1992). Our data suggest that NO regulates NSF by covalently modifying cysteine residues of NSF C91 and C264. How might nitrosylation of C91 or C264 inhibit NSF? Since NO inhibits NSF disassembly activity but

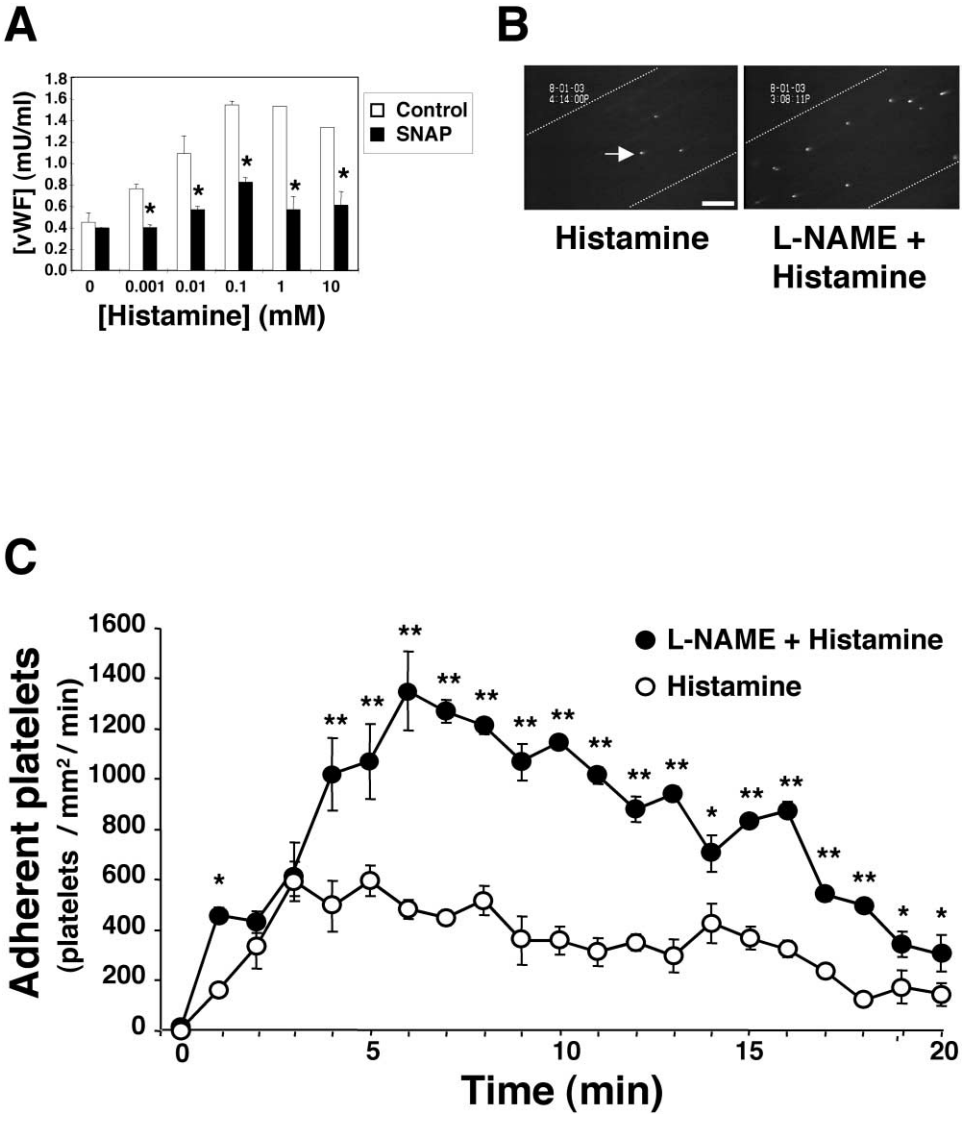


Figure 7. NO Inhibits Exocytosis In Vivo and Consequently Platelet Adhesion to Endothelium

(A) Exogenous NO inhibits histamine induced exocytosis in vitro. HAEC were pretreated with the NO donor SNAP 100 μM for 4 hr and then stimulated with histamine for 1 hr, and the amount of released vWF was measured as above ($n = 2 \pm$ SD, *$p < 0.05$ versus 0 μM).

(B) Inhibition of endogenous NOS increases histamine induced platelet adherence to venules in mice. Mice were pretreated or not with 5 mg/kg L-NAME for 30 min and then transfused with calcein-AM labeled platelets. Intravital microscopy was used to visualize fluorescent platelets adhering to mesenteric venules 5 min after superfusion with 10 μl of 1 mM histamine. The dotted line indicates the edge of the mesenteric venule. The arrow points to a fluorescent platelet adhering to the vessel wall (bar = 50 μm).

(C) Inhibition of endogenous NOS increases platelet adherence to venules in mice over time. Mice were pretreated (black circles) or not (white circles) with L-NAME and then transfused with calcein-AM labeled platelets as above. Intravital microscopy was used to visualize fluorescent platelets transiently adhering to mesenteric venules 0–20 min after superfusion with 10 μl of 1 mM histamine. Quantitative analysis of platelet adhesion as a function of time after the secretagogue application is shown ($n = 4$–5 mice $\pm$ SEM, *$p < 0.05$ and **$p < 0.01$ versus nontreated).

does not affect NSF ATPase activity, NO may uncouple the ability of NSF to convert the chemical energy of ATP hydrolysis into the mechanical energy necessary to separate the SNARE complex. NSF C91 is not adjacent to the N-terminal-D1 region linker, where its modification might influence a conformational change of NSF. However, NSF C264 is located within the D1 domain Walker A motif, which interacts with ATP, and it is possible that nitrosylation of C264 may affect the efficiency by which ATP hydrolysis is converted into mechanical energy.

### Importance of Cysteine Residues to NSF Function

Our data emphasize the importance of cysteine residues to the function of NSF. Specific cysteine residues play a role in ATP hydrolysis: mutation of C21, C91, C264, and C334 reduces the ATPase activity of NSF by approximately 50% (Figure 4B). C264 is located within the Walker A motif of the D1 domain, and C334 is located three residues away from the Walker B motif of the D1 domain, so mutation of these residues may alter ATP binding or hydrolysis. Specific cysteine residues C11, C21, C334, C568, and C582 are necessary for NSF to

interact with the SNARE complex. Mutation of C11 and C21 in the N-terminal domain may interfere with the ability of NSF to interact with α-SNAP. Mutation of the cysteine residues C334 in the D1 domain and C568 and C582 in the D2 domain may affect the structure of NSF necessary for interaction with SNARE molecules. Finally, cysteine residues C91 and C264 are necessary for NSF to disassemble the SNARE complex.

## How Does NO Inhibition of NSF Inhibit Exocytosis?

NO inhibition of NSF is a mechanism by which NO can regulate exocytosis. NSF is required for vesicle trafficking, although the precise stage at which it acts is unclear. NSF was originally thought to prime vesicles for fusion with target membranes. NSF activity is required prior to exocytosis in *Drosophila* (Littleton and Bellen, 1995; Littleton et al., 1998). The NSF homolog Sec18 is necessary prior to vacuole fusion in yeast (Mayer and Wickner, 1997; Mayer et al., 1996; Nichols et al., 1997). Finally, NSF and ATP are necessary for the incorporation of the rab effector EEA1 into the SNARE complex, which may mediate vesicle tethering prior to fusion (McBride et al., 1999). However, more recent data suggests that NSF regulates vesicle trafficking after fusion, disassembling the SNARE complex to permit recycling of individual SNARE molecules (Burgoyne and Morgan, 1998). It is also possible that NSF may play distinct roles in different organisms or that NSF may regulate multiple stages of vesicle transport. Whether NSF regulates vesicle trafficking prior to or following membrane fusion, NSF is necessary for membrane fusion, and NO inhibition of NSF is a mechanism by which NO can regulate exocytosis.

## Implications for Regulation of Exocytosis

NO inhibition of NSF is one possible mechanism for the anti-inflammatory effects of NO. NO derived from NOS3 in endothelial cells or NOS2 in macrophages can nitrosylate and inhibit NSF, decreasing Weibel-Palade body exocytosis, and limiting leukocyte rolling and activation. Conversely, lack of NO and increased Weibel-Palade body exocytosis may explain in part the increased risk for vascular inflammation and atherosclerosis in patients with impaired vascular NO synthesis. Finally, our observations may have significance for other areas of biology as well. NO nitrosylation of NSF may be a mechanism for regulation of a variety of physiological processes mediated by granule exocytosis, including neurotransmission, platelet thrombosis, and cytotoxic T lymphocyte killing.

## Experimental Procedures

### Materials

Thrombin was purchased from Enzyme Research Laboratories (South Bend, IN). Diethylamine (DEA)-NONOate and dithylenetriamine (DETA)-NONOate were purchased from Cayman Chemical (Ann Arbor, MI). Calcein-acetoxymethylester was purchased from Molecular Probes (Eugene, OR). Mouse monoclonal antibody to syntaxin-4 was from BD Biosciences (Bedford, MA). Rabbit polyclonal antibodies to NSF (H-300), α-SNAP (FL-295), and VAMP (FL-118) were from Santa Cruz Biotechnology, Inc. (Santa Cruz, CA). The antibody to nitrosocysteine was from Calbiochem (San Diego, CA). The cDNAs of RGS-$His_6$-NSF and RGS-$His_6$-α-SNAP were generous gifts from James E. Rothman (Rockefeller University, NY). Mice were purchased from Jackson Laboratories (Bar Harbor, ME).

### Peptides

Peptides were synthesized by Anaspec, Inc. (San Jose, CA). The TAT-NSF222 fusion polypeptide sequence is: YGRKKRRQRRRGG-GLDKEFNSIFRRAFASRVFPPE. The control peptide TAT-NSF222scr sequence is: YGRKKRRQRRRGG-GENSFRFLADIFPAKAFPVRFE.

### Preparation of Recombinant NSF and SNARE Polypeptides

Recombinant RGS-$(His)_6$-NSF and RGS-$(His)_6$-α-SNAP were expressed in bacteria and purified on a Ni-NTA-agarose column (His-TRAP, Amersham, Uppsala, Sweden). Recombinant GST-SNARE proteins were expressed in BL21 cells and purified with glutathione-agarose (GSTrap, Amersham). For some assays, the GST tag was cleaved off of the GST-SNARE polypeptide with thrombin.

### Cell Culture and Analysis of vWF Release

Human aortic endothelial cells (HAEC) and EGM-2 media were obtained from Clonetics (Walkersville, MD). HAEC were pretreated with NO donors, washed, stimulated with 1 U/ml of thrombin, and the amount of vWF released into the media was measured by an ELISA (American Diagnostica, Greenwich, CT). HAEC were permeabilized by incubation with 10 U/well of SLO (Sigma) in PBS pH 7.4 for 15 min at 37°C (Walev et al., 2001). Some cells were incubated with 20–200 μg/ml of antibodies or with 100 μg/ml of recombinant NSF. Cells were then resealed by incubation with EGM-2 media for 4 hr at 37°C, washed with EGM-2 media, and stimulated with thrombin as above.

### ATPase Assay

The ATPase activity of NSF was measured by a coupled assay in which ATP utilization is linked to the pyruvate kinase reaction, which generates pyruvate, which in turn is measured continuously with lactate dehydrogenase (Huang and Hackney, 1994). Recombinant NSF (0.2 μg/μl) was pretreated with buffer or DEA or DEA-NONOate or NEM for 10 min at 22°C. ATPase reaction buffer (100 mM HEPES buffer [pH 7.0], 100 mM KCl, 10 mM $MgCl_2$, 5 mM $CaCl_2$, 10 mM ATP, 5 mM phosphoenol pyruvate, 50 U lactate dehydrogenase, and 50 U pyruvate kinase) was added to the mixture, followed by 10 μl of NADH (2 mg/ml in 1% sodium bicarbonate). The mixture was incubated for 10 min at 22°C, and the absorbance was measured at 340 nm.

### NSF Disassembly Assay

Analysis of the 7S and 20S complexes was performed according to previously published protocols (Sollner et al., 1993). The disassembly activity of NSF was measured by a coprecipitation assay (Pevsner et al., 1994). Recombinant RGS-$(His)_6$-NSF (0.1 μg/μl) was pretreated with buffer or 1.0 mM DEA or DEA-NONOate for 10 min at 22°C. Recombinant RGS-$(His)_6$-α-SNAP (0.1 μg/μl), and SNARE polypeptides (0.1 μg/μl each of VAMP-3, SNAP-23, and GST-Syntaxin-4) were added, followed by either 5 mM ATP/10 mM $MgCl_2$ or 5 mM ATP-γS/10 mM $MgCl_2$. This mixture of NSF and SNARE polypeptides was then incubated in binding buffer (4 mM HEPES pH 7.4, 0.1M NaCl, 1 mM EDTA, 3.5 mM $CaCl_2$, 3.5mM $MgCl_2$, and 0.5% Nonidet P-40) and glutathione-sepharose beads for 1 hr at 4°C with rotation. The beads were washed with binding buffer 4 times, mixed with SDS-PAGE sample buffer, boiled for 3 min, and analyzed by immunoblotting.

### Determination of S-Nitrosylation of NSF

Measurement of cysteine residues nitrosylated in vitro was performed by the Saville and Griess assays (Saura et al., 1999). Measurement of NSF nitrosylated in cultured cells was performed by immunoprecipitation with antibody to nitrosocysteine, followed by immunoblotting with antibody to NSF. Measurement of cysteine residues nitrosylated in vivo was performed as previously (Jaffrey et al., 2001; Jaffrey and Snyder, 2001).

### Bleeding Times in Mice

Measurement of bleeding time in mice was performed as previously described (Weiss et al., 2002). Mice were anesthetized with an intra-

muscular injection of ketamine and xylazine, and 5 mm of the distal tip of the tail was amputated. The tail was blotted with filter paper every 5 s until the paper was no longer stained. If the animals bled for 20 min, the experiment was stopped, and the bleeding time was recorded as 20 min.

### Platelet Adherence to Venules in Mice

Measurements of platelet adherence in mice was adapted from Andre et al. (2000). Mice were injected or not with 5 mg/kg L-NAME intravenously, and after 30 min, transfused with calcein-acetoxymethylester (calcein-AM)-labeled murine platelets (Denis et al., 1998). The animals were then prepared for intravital microscopy with an externalized mesentery (Ni et al., 2000). One mesenteric venule (130–180 μm in diameter) per animal was filmed for 2 min before and 20 min after a topical superfusion of 10 μl of 1 mM histamine. Platelet adherence was expressed as the number of adhering fluorescent cells per square millimeter of venular surface, calculated from the diameter and length of segment viewed.

### Acknowledgments

This work was supported by grants from the NIH (R01 HL63706-04, R01 HL074061, P01 HL65608, P01 HL56091), AHA (EIG 0140210N), the Ciccarone Center, and the John and Cora H. Davis Foundation to C.J.L.; by grants from the NIH NHLBI (R37 HL41002) to D.D.W.; by grants from the NIH to J.P.; and by grants RR07002 and HL074945 from the NIH to C.N.M.

Received: December 2, 2002
Revised: September 11, 2003
Accepted: September 11, 2003
Published: October 16, 2003

### References

Andre, P., Denis, C.V., Ware, J., Saffaripour, S., Hynes, R.O., Ruggeri, Z.M., and Wagner, D.D. (2000). Platelets adhere to and translocate on von Willebrand factor presented by endothelium in stimulated veins. Blood *96*, 3322–3328.

Becker-Hapak, M., McAllister, S.S., and Dowdy, S.F. (2001). TAT-mediated protein transduction into mammalian cells. Methods *24*, 247–256.

Block, M.R., Glick, B.S., Wilcox, C.A., Wieland, F.T., and Rothman, J.E. (1988). Purification of an N-ethylmaleimide-sensitive protein catalyzing vesicular transport. Proc. Natl. Acad. Sci. USA *85*, 7852–7856.

Bonfanti, R., Furie, B.C., Furie, B., and Wagner, D.D. (1989). PADGEM (GMP140) is a component of Weibel-Palade bodies of human endothelial cells. Blood *73*, 1109–1112.

Burgoyne, R.D., and Morgan, A. (1998). Analysis of regulated exocytosis in adrenal chromaffin cells: insights into NSF/SNAP/SNARE function. Bioessays *20*, 328–335.

Christopherson, K.S., and Bredt, D.S. (1997). Nitric oxide in excitable tissues: physiological roles and disease. J. Clin. Invest. *100*, 2424–2429.

Denis, C., Methia, N., Frenette, P.S., Rayburn, H., Ullman-Cullere, M., Hynes, R.O., and Wagner, D.D. (1998). A mouse model of severe von Willebrand disease: defects in hemostasis and thrombosis. Proc. Natl. Acad. Sci. USA *95*, 9524–9529.

Huang, T.G., and Hackney, D.D. (1994). Drosophila kinesin minimal motor domain expressed in Escherichia coli. Purification and kinetic characterization. J. Biol. Chem. *269*, 16493–16501.

Huber, D., Cramer, E.M., Kaufmann, J.E., Meda, P., Masse, J.M., Kruithof, E.K., and Vischer, U.M. (2002). Tissue-type plasminogen activator (t-PA) is stored in Weibel-Palade bodies in human endothelial cells both in vitro and in vivo. Blood *99*, 3637–3645.

Jaffrey, S.R., and Snyder, S.H. (2001). The biotin switch method for the detection of s-nitrosylated proteins. Sci STKE 2001: pl1 [DOI:10.1126/stke.2001.86.pl1].

Jaffrey, S.R., Erdjument-Bromage, H., Ferris, C.D., Tempst, P., and Snyder, S.H. (2001). Protein S-nitrosylation: a physiological signal for neuronal nitric oxide. Nat. Cell Biol. *3*, 193–197.

Jahn, R., and Sudhof, T.C. (1999). Membrane fusion and exocytosis. Annu. Rev. Biochem. *68*, 863–911.

Jahn, R., Lang, T., and Sudhof, T.C. (2003). Membrane fusion. Cell *112*, 519–533.

Kaiser, C.A., and Schekman, R. (1990). Distinct sets of SEC genes govern transport vesicle formation and fusion early in the secretory pathway. Cell *61*, 723–733.

Kuhlencordt, P.J., Chen, J., Han, F., Astern, J., and Huang, P.L. (2001a). Genetic deficiency of inducible nitric oxide synthase reduces atherosclerosis and lowers plasma lipid peroxides in apolipoprotein E-knockout mice. Circulation *103*, 3099–3104.

Kuhlencordt, P.J., Gyurko, R., Han, F., Scherrer-Crosbie, M., Aretz, T.H., Hajjar, R., Picard, M.H., and Huang, P.L. (2001b). Accelerated atherosclerosis, aortic aneurysm formation, and ischemic heart disease in apolipoprotein E/endothelial nitric oxide synthase double-knockout mice. Circulation *104*, 448–454.

Littleton, J.T., and Bellen, H.J. (1995). Presynaptic proteins involved in exocytosis in Drosophila melanogaster: a genetic analysis. Invert. Neurosci. *1*, 3–13.

Littleton, J.T., Chapman, E.R., Kreber, R., Garment, M.B., Carlson, S.D., and Ganetzky, B. (1998). Temperature-sensitive paralytic mutations demonstrate that synaptic exocytosis requires SNARE complex assembly and disassembly. Neuron *21*, 401–413.

Malhotra, V., Orci, L., Glick, B.S., Block, M.R., and Rothman, J.E. (1988). Role of an N-ethylmaleimide-sensitive transport component in promoting fusion of transport vesicles with cisternae of the Golgi stack. Cell *54*, 221–227.

May, A.P., Whiteheart, S.W., and Weis, W.I. (2001). Unraveling the mechanism of the vesicle transport ATPase NSF, the N-ethylmaleimide-sensitive factor. J. Biol. Chem. *276*, 21991–21994.

Mayadas, T.N., Johnson, R.C., Rayburn, H., Hynes, R.O., and Wagner, D.D. (1993). Leukocyte rolling and extravasation are severely compromised in P selectin-deficient mice. Cell *74*, 541–554.

Mayer, A., and Wickner, W. (1997). Docking of yeast vacuoles is catalyzed by the Ras-like GTPase Ypt7p after symmetric priming by Sec18p (NSF). J. Cell Biol. *136*, 307–317.

Mayer, A., Wickner, W., and Haas, A. (1996). Sec18p (NSF)-driven release of Sec17p (alpha-SNAP) can precede docking and fusion of yeast vacuoles. Cell *85*, 83–94.

McBride, H.M., Rybin, V., Murphy, C., Giner, A., Teasdale, R., and Zerial, M. (1999). Oligomeric complexes link Rab5 effectors with NSF and drive membrane fusion via interactions between EEA1 and syntaxin 13. Cell *98*, 377–386.

McEver, R.P., Beckstead, J.H., Moore, K.L., Marshall-Carlson, L., and Bainton, D.F. (1989). GMP-140, a platelet alpha-granule membrane protein, is also synthesized by vascular endothelial cells and is localized in Weibel-Palade bodies. J. Clin. Invest. *84*, 92–99.

Mellman, I., and Warren, G. (2000). The road taken: past and future foundations of membrane traffic. Cell *100*, 99–112.

Michel, T., and Feron, O. (1997). Nitric oxide synthases: which, where, how, and why? J. Clin. Invest. *100*, 2146–2152.

Nathan, C., and Xie, Q.W. (1994). Nitric oxide synthases: roles, tolls, and controls. Cell *78*, 915–918.

Ni, H., Denis, C.V., Subbarao, S., Degen, J.L., Sato, T.N., Hynes, R.O., and Wagner, D.D. (2000). Persistence of platelet thrombus formation in arterioles of mice lacking both von Willebrand factor and fibrinogen. J. Clin. Invest. *106*, 385–392.

Nichols, B.J., Ungermann, C., Pelham, H.R., Wickner, W.T., and Haas, A. (1997). Homotypic vacuolar fusion mediated by t- and v-, R.D., and Sessa, W.C. (1999). Molecular control of nitric oxide synthases in the cardiovascular system. SNAREs. Nature *387*, 199–202.

Papapetropoulos, A., Rudic, R.D., and Sessa, W.C. (1999). Molecular control of nitric oxide synthases in the cardiovascular system. Cardiovasc. Res. *43*, 509–520.

Pevsner, J., Hsu, S.C., and Scheller, R.H. (1994). n-Sec1: a neural-specific syntaxin-binding protein. Proc. Natl. Acad. Sci. USA *91*, 1445–1449.

Qian, Z., Gelzer-Bell, R., Yang Sx, S.X., Cao, W., Ohnishi, T., Wasowska, B.A., Hruban, R.H., Rodriguez, E.R., Baldwin, W.M., 3rd, and Lowenstein, C.J. (2001). Inducible nitric oxide synthase inhibition of Weibel-Palade body release in cardiac transplant rejection. Circulation *104*, 2369–2375.

Radomski, M.W., and Moncada, S. (1993). Regulation of vascular homeostasis by nitric oxide. Thromb. Haemost. *70*, 36–41.

Rothman, J.E., and Wieland, F.T. (1996). Protein sorting by transport vesicles. Science *272*, 227–234.

Rudic, R.D., Shesely, E.G., Maeda, N., Smithies, O., Segal, S.S., and Sessa, W.C. (1998). Direct evidence for the importance of endothelium-derived nitric oxide in vascular remodeling. J. Clin. Invest. *101*, 731–736.

Ruggeri, Z.M. (1997). von Willebrand factor. J. Clin. Invest. *100*, S41–S46.

Saura, M., Zaragoza, C., McMillan, A., Quick, R.A., Hohenadl, C., Lowenstein, J.M., and Lowenstein, C.J. (1999). An antiviral mechanism of nitric oxide: inhibition of a viral protease. Immunity *10*, 21–28.

Schweizer, F.E., Dresbach, T., DeBello, W.M., O'Connor, V., Augustine, G.J., and Betz, H. (1998). Regulation of neurotransmitter release kinetics by NSF. Science *279*, 1203–1206.

Sollner, T., Whiteheart, S.W., Brunner, M., Erdjument-Bromage, H., Geromanos, S., Tempst, P., and Rothman, J.E. (1993). SNAP receptors implicated in vesicle targeting and fusion. Nature *362*, 318–324.

Springer, S., Spang, A., and Schekman, R. (1999). A primer on vesicle budding. Cell *97*, 145–148.

Stamler, J.S. (1994). Redox signaling: nitrosylation and related target interactions of nitric oxide. Cell *78*, 931–936.

Stamler, J.S., Singel, D.J., and Loscalzo, J. (1992). Biochemistry of nitric oxide and its redox-activated forms. Science *258*, 1898–1902.

Stamler, J.S., Lamas, S., and Fang, F.C. (2001). Nitrosylation. the prototypic redox-based signaling mechanism. Cell *106*, 675–683.

Vischer, U.M., and Wagner, D.D. (1993). CD63 is a component of Weibel-Palade bodies of human endothelial cells. Blood *82*, 1184–1191.

Wagner, D.D. (1993). The Weibel-Palade body: the storage granule for von Willebrand factor and P-selectin. Thromb. Haemost. *70*, 105–110.

Wagner, D.D., Olmsted, J.B., and Marder, V.J. (1982). Immunolocalization of von Willebrand protein in Weibel-Palade bodies of human endothelial cells. J. Cell Biol. *95*, 355–360.

Walev, I., Bhakdi, S.C., Hofmann, F., Djonder, N., Valeva, A., Aktories, K., and Bhakdi, S. (2001). Delivery of proteins into living cells by reversible membrane permeabilization with streptolysin-O. Proc. Natl. Acad. Sci. USA *98*, 3185–3190.

Weibel, E.R., and Palade, J.E. (1964). New cytoplasmic components in arterial endothelium. J. Cell Biol. *23*, 101–106.

Weiss, E.J., Hamilton, J.R., Lease, K.E., and Coughlin, S.R. (2002). Protection against thrombosis in mice lacking PAR3. Blood *100*, 3240–3244.

Wickner, W., and Haas, A. (2000). Yeast homotypic vacuole fusion: a window on organelle trafficking mechanisms. Annu. Rev. Biochem. *69*, 247–275.